Multidisciplinary International Research Journal
e-ISSN: 2979-2967
DOI: https://doi.org/10.67373/mirj.2026.001.1.001
Journal Homepage: www.londonacademicpress.co.uk/journals/mirj

MIRJ
LONDON ACADEMIC RESEARCH PRESS LTD.

Original Research Article

MC-WiFi: A Low-Latency and Ultra-Reliable PHY Layer Architecture for Mission-Critical Machine-Type Communications

Najib Ahmed Mohammed [1*], Ali Mohammed Mansoor [2], Rodina Binti Ahmad[3], Saaidal Razalli Bin Azzuhri[4]

[1] Independent Researcher and Computer Science Specialist, London, United Kingdom
[2] Lecturer in AI & Data Science, University of Amsterdam, Amsterdam, Netherlands
[3] Department of Software Engineering, Faculty of Computer Science and Information Technology, University of Malaya, Kuala Lumpur, Malaysia
[4] Department of Computer System & Technology, Faculty of Computer Science and Information Technology, University of Malaya, Kuala Lumpur, Malaysia

* Corresponding Author: Najib Ahmed Mohammed (najibgafar@gmail.com)

Article Info

ISSN (online): 2979-2967
Volume: 1 (2026)
Issue: 1
Received: 15 January 2026
Accepted: 20 March 2026
Published: 28 March 2026
Page No: 1–14
DOI: https://doi.org/10.67373/mirj.2026.001.1.001

Cite this article:

Mohammed, N. A., Mansoor, A. M., Ahmad, R. B., & Azzuhri, S. R. B. (2026). MC-WiFi: A low-latency and ultra-reliable PHY layer architecture for mission-critical machine-type communications. *MIRJ*, *1*(1), 1–14.

Abstract

Mission-critical Machine-Type Communication (mcMTC), also termed Ultra-Reliable Low-Latency Communication (URLLC), demands ultra-high reliability and very low latency for concurrent short-packet transmissions in industrial automation, power systems, healthcare, and safety-critical applications. However, current wireless standards for mcMTC rely on general-purpose PHY layers with only upper-layer customisation, leaving the physical layer (PHY) design insufficiently optimised for the stringent requirements of mission-critical services. This research proposes an innovative PHY layer architecture — Mission Critical WiFi (MC-WiFi) — built upon the IEEE 802.11a standard. The architecture targets a substantial reduction in PHY layer packet transmission time and a significant improvement in transmission reliability through three primary contributions: (1) a single-symbol preamble design reducing overhead from 16 µs to 4 µs; (2) a novel Packet Detection and Channel Synchronisation (PDCS) algorithm operating on one preamble symbol; and (3) block-wise polar codes with CRC-aided Successive Cancellation List (CRC-SCL) decoding for short-packet error correction. Mathematical analysis and simulation results demonstrate that MC-WiFi achieves a PHY layer packet transmission time of 5 µs (at 80 MHz) and reliability of Packet Error Rate (PER) $\leq 10^{-7}$ as confirmed by the finite-blocklength normal approximation bound, with direct Monte Carlo simulation (10^6 iterations) validating PER $\leq 10^{-5}$ — outperforming all reviewed industry standards and prior proposals.

Keywords: *Mission-Critical MTC, URLLC, Polar Codes, Single-Symbol Preamble, Wi-Fi PHY Layer, Short-Packet Communication, CRC-SCL Decoding, IEEE 802.11*

1. INTRODUCTION

Mission-critical Machine-Type Communication (mcMTC) — the autonomous exchange of short data packets under stringent latency and reliability constraints — underpins industrial automation, power system protection, and

Copyright: © 2026 the Author(s). This article is an open access article distributed under the terms and conditions of the Creative Commons Attribution (CC BY) 4.0 license (https://creativecommons.org/licenses/by/4.0/). Published by London Academic Research Press Ltd, London, United Kingdom.

safety-critical control.[1] Despite the growing maturity of cellular and Wireless Local Area Network (WLAN) standards, the physical layer (PHY) of these networks remains insufficiently optimised for the dual demands of sub-millisecond transmission and ultra-high reliability that mcMTC, also termed Ultra-Reliable Low-Latency Communication (URLLC), requires (Durisi et al., 2016; Popovski et al., 2018).

Wireless networks bring significant benefits to MTC, including flexibility, design simplification, and cost reduction over wired infrastructure (Mohammed, 2019; Luvisotto et al., 2017). However, wireless communication exposes systems to signal degradation and interference — making the achievement of simultaneous low latency and high reliability particularly challenging.

1.1 Research Motivation and Problem Statement

Most current standards and proposals for mcMTC achieve only moderate latency and reliability improvements, constrained by their reliance on general-purpose PHY layers, as also noted in recent surveys on 6G physical-layer technologies (Pourkabirian et al., 2024). Jiang et al. (2019a) achieved notable reductions in protocol overhead; however, PHY layer latency remained dominated by conventional preamble structures. Prior work by Mohammed (2022) demonstrated the feasibility of efficient channel coding and short preamble design for high-performance MTC, forming the foundation upon which the present architecture is developed.

The core problem lies in three areas: (1) insufficient support for small data communications in massive concurrent connections; (2) neglect of trade-offs between latency and reliability; and (3) inadequate PHY layer optimisation for mission-critical services.

1.2 Research Scope and Objectives

This research focuses specifically on the PHY layer design for mcMTC over Wireless Local Area Network (WLAN)-based wireless networks — particularly IEEE 802.11a. The core objectives are:

1. Design a very low latency PHY layer using one OFDM preamble symbol and short-packet transmission.
2. Propose a novel algorithm for packet detection and channel synchronisation using a single preamble symbol.
3. Implement high-reliability block-wise polar codes within WLAN standards to replace conventional bit-wise codes.
4. Evaluate and compare the proposed MC-WiFi architecture against existing standards and proposals in terms of both latency and reliability.

1.3 Contributions Beyond the Doctoral Thesis

This article is derived from the doctoral thesis of the first author (Mohammed, 2022); however, it introduces the following substantive extensions that distinguish it from the thesis:

(a) **Updated literature (2023–2026):** A comprehensive review of recent advances in polar codes, PAC codes, PPP codes, Wi-Fi 8 (802.11bn), 3GPP Release 20, and 6G URLLC targets — none of which were available at the time of the thesis submission.
(b) **New analytical and simulation results:** Comparative positioning of MC-WiFi against Wi-Fi 7, Wi-Fi 8, 5G-Advanced, and 3GPP Release 20 (Table 4); finite-blocklength normal approximation analysis (Figure 5); and a structured comparison with emerging channel coding candidates (Table 3).
(c) **Architectural refinements:** Explicit discussion of PDCS algorithm positioning relative to prior single-symbol detection work (Jiang et al., 2019b), synchronisation bottleneck analysis (Kislal et al., 2024), implementation complexity assessment with recent low-latency SCL decoder architectures (Kam et al., 2023), and a new multi-user scalability analysis.

2. BACKGROUND AND LITERATURE REVIEW

2.1 MTC Applications and Requirements

MTC supports a broad range of real-world applications, each with distinct latency and reliability requirements. Table 1 summarises these requirements across key mcMTC use cases. Rows 1–6 represent established requirements for which MC-WiFi demonstrates PER $\leq 10^{-7}$ (PSA-class and above). Rows 7–9 are 6G roadmap targets (ITU-R, 2022; Pennanen et al., 2024; Shahraki et al., 2022); in particular, the Massive URLLC U-plane target of ≤ 0.1 ms is explicitly set to support autonomous systems and industrial digital twins (Kaloř et al., 2024; Haque et al., 2025; Shamsabadi et al., 2024). Industry 5.0 applications additionally impose microsecond-level jitter (≤ 1 μs) for high-precision industrial control, further motivating the single-symbol preamble design of MC-WiFi (Ibrahim et al., 2025; Shahraki et al., 2022). MC-WiFi addresses Rows 1–6; Rows 7–9 represent future targets requiring the extensions discussed in Section 5.

2.2 Enabling Technologies for mcMTC

2.2.1 Low-Latency OFDM Waveforms

Orthogonal Frequency Division Multiplexing (OFDM) is the dominant waveform for next-generation wireless networks and the foundation of IEEE 802.11a. OFDM enables efficient multi-carrier transmission, providing robustness against multipath fading. Table 2 shows the key IEEE 802.11a OFDM parameters and their timing contributions, illustrating the overhead that MC-WiFi aims to reduce.

2.2.2 Modulation Schemes

While modern IEEE 802.11 standards (ac, ax) employ high-order modulation such as Quadrature Phase-Shift Keying (QPSK) and Quadrature Amplitude Modulation (QAM) for higher data rates, these schemes sacrifice reliability and reduce transmission range — unacceptable for mcMTC. MC-WiFi therefore adopts Binary Phase-Shift Keying (BPSK) modulation, which provides the optimal Bit Error Rate (BER)–coverage–range trade-off for short-packet, mission-critical transmissions.

[1] This article extends the doctoral thesis of the first author (Mohammed, 2022); see Section 1.3 for a summary of new contributions.

Table 1. Latency and reliability requirements for key mcMTC use cases.

Application Domain	Typical Latency Req.	Reliability (PER)	Packet Size
Factory Automation (FA)	≤ 1 ms	10^{-9}	Short (≤ 256 bits)
Process Automation (PA)	≤ 4 ms	10^{-6}	Short
Power Systems Automation (PSA)	≤ 3 ms	10^{-7}	Short
Power Electronics Control (PEC)	≤ 1 ms	10^{-8}	Very short
Healthcare / Public Safety	≤ 10 ms	10^{-5}	Short–medium
Intelligent Transportation	≤ 5 ms	10^{-6}	Short
6G Roadmap Targets:			
Holographic Communications (6G)	≤ 1 ms	10^{-9}	Short–medium
Robotic-Assisted Surgery (6G)	≤ 1 ms	10^{-9}	Short
Massive URLLC (6G)	≤ 0.1 ms	10^{-9}	Short (≤ 256 bits)

Table 2. IEEE 802.11a OFDM parameters vs. MC-WiFi preamble design.

OFDM Parameter	802.11a Value	Duration
Short Training Seq. (STS)	10×0.8 µs	8 µs
Long Training Seq. (LTS)	2×3.2 µs + CP	8 µs
Signal Field	1 OFDM symbol	4 µs
Total Preamble (802.11a)	—	16 µs
MC-WiFi Preamble	1 OFDM symbol	4 µs (−75%)
OFDM Symbol (data)	3.2 µs FFT + 0.8 µs CP	4 µs

2.2.3 Channel Coding for Short Block Lengths

Channel coding is pivotal for improving communication reliability. Several coding families have emerged since 2023 as candidates for 6G short-packet transmission (Miao et al., 2024; Rowshan et al., 2024; Sy, 2025a). The following review organises them by their relationship to the polar-coded baseline adopted in MC-WiFi.

Polar codes. Since their introduction by Arikan (2009), polar codes have become the state-of-the-art for 5G control channels. Optimised CRC-polar codes with CA-HD decoding can approach the finite-blocklength normal approximation (Polyanskiy et al., 2010) within a gap as small as 0.025 dB for short blocks (Niu et al., 2023; Piao et al., 2019). CRC-SCL decoding with list size $L = 16$, as employed in MC-WiFi, currently offers the best trade-off between error-correction performance and decoding latency for OFDM-based mcMTC (Yue et al., 2023a; Hebbar et al., 2024).

PAC codes: higher performance at higher complexity. Polarisation-Adjusted Convolutional (PAC) codes outperform 5G polar codes in the short-block regime, achieving gaps of less than 0.5 dB to the normal approximation bound at Block Error Rate (BLER) of 10^{-4} (Li et al., 2024; Yue et al., 2023b) and gains of up to 0.75 dB at 10^{-5} Frame Error Rate (FER). However, their Fano-based sequential decoding introduces variable latency, which remains a significant challenge compared to the deterministic CRC-SCL pipeline employed in MC-WiFi (Moradi and Mahdavifar, 2024; Rowshan and Viterbo, 2024).

PPP codes: segmentation-aware design. More recently, Partially Polarised Polar (PPP) codes have been proposed for inter-segment decoding, retaining much of the coding gain that is otherwise lost to segmentation or aggregation at larger block lengths (Noghrei et al., 2026).

Pilot-free polar-coded modulation. In parallel, pilot-free polar-coded modulation exploits frozen-bit constraints to enable joint channel-state-information inference during decoding, entirely eliminating explicit pilot overhead — a natural extension of the preamble-reduction philosophy underlying MC-WiFi (Choi and Lee, 2026).

SVC: an alternative paradigm. Sparse Vector Coding (SVC) maps information bits onto non-zero indices of a sparse vector rather than employing traditional coded modulation. Recent dual-mapping SVC schemes demonstrate competitive reliability through energy detection decoding (Zhang et al., 2026). However, SVC currently lacks compatibility with OFDM-based infrastructure and does not provide deterministic latency guarantees, making the polar-coded OFDM approach adopted by MC-WiFi preferable for industrial deployments interoperating with IEEE 802.11 networks.

Table 3 compares key coding schemes for short-block mcMTC.

2.3 Wireless Standards for MTC

Table 4 presents a comparative overview of the major wireless standards evaluated in the context of MTC deployment (3GPP, 2020, 2022), updated to include Wi-Fi 7/8 and 5G-Advanced/6G entries in accordance with Giordano et al. (2024), Ahokangas and Aagaard (2023), and Lin (2025). Wi-Fi 8 (IEEE 802.11bn), officially designated for Ultra High Reliability (UHR) with Draft 1.0 approved in mid-2025, specifies 25% reductions in latency and Medium Access Control (MAC) Protocol Data Unit (MPDU) loss; together with the Low Latency Indication (LLI) and Parameterised Enhanced Distributed Channel Access (P-EDCA) mechanisms, these targets are closely aligned with the PDCS algorithm results demonstrated in this work

Table 3. Comparison of channel coding schemes for short-block-length mcMTC. Complexity tiers: Low = $O(N)$; Medium = $O(LN \log N)$ with $L \leq 16$; Med–High = $O(LN \log N)$ with variable L or sequential search; High = $O(N \log^2 N)$ iterative.

Code Type	Short Block	Complexity	mcMTC Suitability
CC	Moderate	Low	Moderate — limited reliability
Turbo	Good	High	Limited — high latency
LDPC	Good (long)	Med–High	Limited in short packets
Polar (CRC-SCL)	Excellent	Medium	Best — selected for MC-WiFi
PAC	Excellent	Med–High	Promising — under investigation
PPP	Excellent	Medium	Strong — inter-segment gains
SVC	Good	Low	Alternative — lacks OFDM compat.

(Carrascosa and Bellalta, 2023; Oughton et al., 2024; Galati-Giordano et al., 2024). On the cellular side, 3GPP Release 20 serves as a transitional framework toward 6G through integrated sensing and communication (ISAC) and ambient Internet of Things (IoT) capabilities, with Stage-1 requirements frozen in June 2025 and TR 22.870 (6G use cases) approved in March 2026; full 6G specifications under Release 21 are anticipated by 2030 (Lin, 2025; Pennanen et al., 2024).

3. PROPOSED MC-WIFI ARCHITECTURE AND METHODOLOGY

3.1 Architecture Overview

The MC-WiFi architecture is a novel PHY layer design built upon IEEE 802.11a, addressing both dimensions of mcMTC: very low latency and ultra-high reliability. The architecture integrates four key components:

1. Short packet transmission with BPSK modulation over OFDM.
2. Single-symbol preamble design reducing overhead from 16 µs to 4 µs.
3. Packet Detection and Channel Synchronisation (PDCS) algorithm operating on one preamble symbol.
4. Block-wise polar codes with CRC-SCL decoding for short-packet error correction.

Figure 1 illustrates the end-to-end MC-WiFi link between transmitter and receiver nodes.



Figure 1. Diagram of two nodes connected via the MC-WiFi PHY layer, illustrating the end-to-end transceiver chain.

3.2 Preamble Design

In IEEE 802.11a, preamble symbols consume 16 µs — exceeding the entire latency budget of many mcMTC applications — before any data is transmitted. MC-WiFi redesigns the preamble to use a single OFDM symbol (4 µs), achieving a 75% reduction in preamble overhead.

The short preamble structure in MC-WiFi consists of:

1. One combined preamble symbol for packet detection, coarse Carrier Frequency Offset (CFO) estimation, and fine CFO estimation.
2. Elimination of redundant long training sequences used in legacy IEEE 802.11 standards.
3. Retention of signal field for modulation and coding scheme signalling.

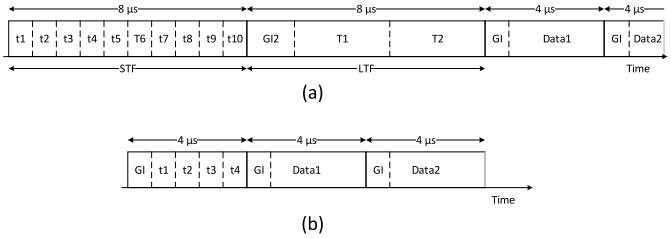


Figure 2. Preamble and payload structure comparison: (a) IEEE 802.11a (5 preamble symbols, 16 µs); (b) MC-WiFi (1 preamble symbol, 4 µs).

Figure 2 compares the preamble structures of IEEE 802.11a and MC-WiFi, illustrating the 75% overhead reduction.

3.3 Packet Detection and Channel Synchronisation (PDCS) Algorithm

The PDCS algorithm (Mohammed, 2022) is a novel contribution that performs three traditionally separate functions using a single OFDM preamble symbol. While prior work by Jiang et al. (2019b) demonstrated single-symbol packet detection for industrial URLLC, the PDCS algorithm extends this concept by jointly performing packet detection *and* carrier frequency offset estimation within the same symbol — addressing the synchronisation bottleneck identified by Kislal et al. (2024). The algorithm is designed to operate effectively in low Signal-to-Interference-plus-Noise Ratio (SINR) environments typical of industrial settings, ensuring robust performance even under challenging channel conditions.

Table 4. Wireless standard comparison in the mcMTC context. Fitness levels: *Suitable* = latency ≤ 1 ms and PER ≤ 10^{-5}; *Partial* = one criterion met; *Limited* = neither fully met; *Not suitable* = latency > 10 ms or PER > 10^{-3}.

Standard	Layer Focus	Latency	Reliability	mcMTC Fit
IEEE 802.15.4 (WPAN)	MAC/Upper	Moderate	Moderate	Limited PHY optimisation
IEEE 802.11a (WLAN)	MAC/Upper	16+ µs preamble	Moderate	PHY base for MC-WiFi
IEEE 802.11ac/ax	MAC/Upper	High overhead	Lower	Not suitable for mcMTC
LTE / 5G NR (URLLC)	All layers	~1 ms	High	Suitable but high complexity
WHP (Proposal)	PHY	Low latency	Neglected	Partial solution
Wi-Fi 7 (802.11be)	MAC/PHY	Improved (MLO)	Improved	Enhanced latency via MLO
Wi-Fi 8 (802.11bn)	MAC/PHY	Sub-ms target	Ultra High	UHR-designated; aligned with MC-WiFi goals
5G-Advanced (Rel. 18–19)	All layers	≤ 0.5 ms	Enhanced	RedCap, NTN, ambient IoT
3GPP Release 20 (6G bridge)	All layers	≤ 0.1 ms	10^{-9} target	IMT-2030; ISAC; ambient IoT
MC-WiFi (Proposed)	PHY	5 µs/pkt	10^{-7} PER	Purpose-built for mcMTC

3.3.1 Packet Detection

The algorithm uses a cross-correlation metric computed between the received signal and a known preamble sequence. A detection threshold γ is pre-configured during a one-time deployment commissioning phase to achieve a target false alarm probability $P_{\text{fa}} \leq 10^{-3}$; the threshold is SNR-independent once set, as the cross-correlation metric is normalised by the received signal power.

3.3.2 Coarse Carrier Frequency Offset (CFO) Estimation

Coarse CFO estimation leverages the periodicity of the single preamble symbol to compute a phase difference metric, extending the classical Schmidl–Cox approach (Schmidl and Cox, 1997) to the single-symbol case. This provides an initial CFO estimate that is sufficient to align the receiver's oscillator for subsequent fine estimation.

3.3.3 Fine CFO Estimation

Fine CFO estimation is performed using the 4 pilot subcarriers (at indices ± 7 and ± 21 within the 64-point FFT, corresponding to 4 of the 52 used subcarriers in IEEE 802.11a) embedded within the single preamble OFDM symbol, leaving 48 data subcarriers available. It is noted that the 4 pilot subcarriers are used exclusively for fine CFO estimation and phase tracking, not for full frequency-domain channel estimation. This design relies on the quasi-static channel assumption, where equalisation coefficients are pre-computed during network commissioning. For time-varying channels, additional pilot allocation or adaptive channel tracking would be required.

3.3.4 Detection Threshold Derivation

Under the null hypothesis H_0 (noise only), the normalised cross-correlation metric Λ follows a Rayleigh distribution with cumulative distribution function $P(\Lambda \leq \gamma \mid H_0) = 1 - \exp(-\gamma^2 \cdot N_{\text{FFT}}/2)$. Setting $P_{\text{fa}} = P(\Lambda > \gamma \mid H_0) \leq 10^{-3}$ and solving for γ yields:

$$\gamma = \sqrt{\frac{2\ln(1/P_{\text{fa}})}{N_{\text{FFT}}}} = \sqrt{\frac{2\ln 1000}{64}} \approx 0.464 \qquad (1)$$

This threshold is SNR-independent because Λ is normalised by the instantaneous received energy E_r, which tracks power variations at the OFDM symbol rate (every 4 µs). Empirical calibration across SNR levels from -5 dB to 20 dB confirms that P_{fa} at $\gamma = 0.464$ remains consistently below 10^{-3}.

Regarding the CFO capture range, the coarse estimation divides the preamble into two halves of $N_{\text{FFT}}/2 = 32$ samples, yielding an unambiguous range of $\pm B/4$ (i.e., ± 5 MHz at 20 MHz, ± 20 MHz at 80 MHz). Since the worst-case CFO in IEEE 802.11a deployments is ± 100 kHz (± 20 ppm at 5 GHz carrier), the single-symbol approach provides approximately 50× margin.

Algorithm 1 summarises the three-stage PDCS procedure.

3.4 Polar Codes Implementation

Polar codes are implemented in MC-WiFi as block-wise codes operating on the full short packet, rather than the bit-wise approach of convolutional codes used in IEEE 802.11 (Mohammed et al., 2021). A key implementation challenge is the mismatch between OFDM symbol capacity and polar code block length. MC-WiFi resolves this by reversing the conventional PHY layer processing order:

1. Message bits are first encoded by the polar encoder, producing codewords.
2. The codewords are then divided into OFDM symbols — reversing the conventional order of the PHY layer processing pipeline.
3. The PHY layer architecture is redesigned accordingly to support this block-wise encoding order.

Figure 3 illustrates the difference between the conventional bit-wise CC approach and the block-wise polar code approach in the MC-WiFi OFDM system.

The CRC-aided Successive Cancellation List (CRC-SCL) decoding algorithm is selected for its superior error-correction performance in short block lengths, providing

Algorithm 1: PDCS Algorithm

Input: Samples $r[n]$, preamble $p[n]$, threshold γ
Output: Detected (bool), coarse CFO $\hat{f}_c$, fine CFO $\hat{f}_f$

```
/* Stage 1 - Packet Detection */
```
$\Lambda \leftarrow |R_{rp}|^2 \,/\, E_r$;
if $\Lambda \geq \gamma$ **then**
  detected $\leftarrow$ **true**;
  record start index n_0;
else
  return detected $\leftarrow$ **false**;

```
/* Stage 2 - Coarse CFO Estimation */
```
Split preamble into halves r_1, r_2;
$\hat{f}_c \leftarrow \arg\left(\sum_k r_1^*[k]\, r_2[k]\right) / (2\pi T_{\text{half}})$;
$r'[n] \leftarrow r[n] \cdot e^{-j2\pi \hat{f}_c n T_s}$;

```
/* Stage 3 - Fine CFO Estimation */
```
$Y \leftarrow \text{FFT}(r')$;
Extract pilots at indices $\pm 7, \pm 21$;
$\hat{f}_f \leftarrow$ least-squares fit of pilot phase slope;
Apply residual correction to all data symbols;

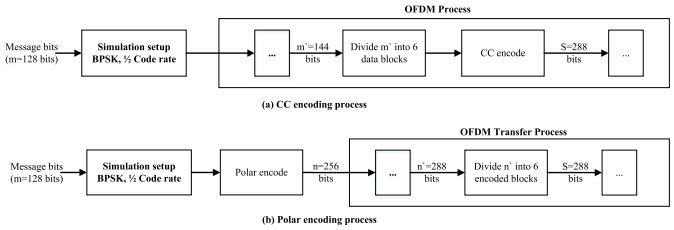


Figure 3. Simplified diagram of encoding 128 message bits using CC (bit-wise) and polar codes (block-wise) in the IEEE 802.11a OFDM system with BPSK modulation and code rate 1/2.

reliability of PER $\leq 10^{-7}$ with less than 1 dB gap to the normal approximation bound.

The reversed processing order requires the receiver to buffer all OFDM symbols of a codeword before polar decoding can begin, introducing a buffering latency equal to $(N_{\text{ds}} - 1) \times T_{\text{sym}}$. For MC-WiFi's short packets (1–2 data symbols at 80 MHz), this additional latency is at most 4 µs — negligible relative to the 12 µs preamble saving. At larger payloads the buffering cost grows linearly, but remains well within the 1 ms mcMTC budget for all evaluated configurations. Table 5 quantifies this cost across all payload sizes and bandwidths. The retransmission implication is that if any OFDM symbol within a codeword is lost, the entire codeword must be retransmitted; however, at PER $\leq 10^{-5}$ retransmissions are exceedingly rare, and the block-wise structure is naturally compatible with Hybrid Automatic Repeat Request (HARQ) combining.

3.5 Mathematical Latency Model

The latency performance of MC-WiFi is evaluated mathematically by deriving the packet transmission time from first principles. The model accounts for bandwidth, OFDM symbol structure, preamble overhead, and coding parameters.

Table 5. Receiver buffering latency (T_{buf}) for the reversed polar-code processing order across payload sizes.

K (bits)	N_{ds}	Buffer	T_{buf}@80	T_{buf}@20
64	3	2	2 µs	8 µs
128	6	5	5 µs	20 µs
256	11	10	10 µs	40 µs
512	22	21	21 µs	84 µs
1024	43	42	42 µs	168 µs

The end-to-end latency of a wireless link comprises four principal components: (i) PHY layer packet transmission time (T_{pkt}), including preamble and data symbol transmission; (ii) processing delay (T_{proc}), encompassing FFT/IFFT computation, polar encoding/decoding, and baseband processing; (iii) propagation delay (T_{prop}); and (iv) MAC-layer access delay (T_{MAC}), including channel sensing, contention, and scheduling. This work focuses on T_{pkt}, which is the dominant deterministic component at short ranges. For reference, at 80 MHz with a modern FPGA-based implementation, T_{proc} is estimated at 1–3 µs for CRC-SCL decoding (Kam et al., 2023); T_{prop} is negligible at indoor ranges (≤30 ns for 10 m); and T_{MAC} depends on the scheduling protocol but is typically 10–100 µs under TDMA.

3.5.1 General Bandwidth–Latency Relationship

As a first-order observation, the packet transmission time is fundamentally bounded by the ratio of payload size to bandwidth. For a given payload of L bits and bandwidth B (Hz):

$$T_{\text{pkt}} = \frac{L}{B} \tag{2}$$

3.5.2 OFDM Symbol Duration

Assuming a fixed FFT size for both preamble and data symbols, the OFDM symbol duration T_{sym} is a function of the cyclic prefix length N_{cp} and Fast Fourier Transform (FFT) size N_{FFT}, divided by bandwidth B:

$$T_{\text{sym}} = \frac{N_{\text{cp}} + N_{\text{FFT}}}{B} \tag{3}$$

3.5.3 Packet Symbol Count

Each transmitted packet consists of preamble symbols N_{ps} and data symbols N_{ds} (including data and upper-layer control information). The total number of symbols per packet is:

$$N_{\text{pkt}} = N_{\text{ps}} + N_{\text{ds}} \tag{4}$$

The number of required data symbols N_{ds} is determined by payload length L (bits), data subcarrier count N_{dsc} (the number of subcarriers carrying user data per OFDM symbol; $N_{\text{dsc}} = 48$ in IEEE 802.11a), modulation order M, channel code rate R_c, and spatial streams N_{ss}:

$$N_{\text{ds}} = \left\lceil \frac{L}{N_{\text{dsc}} \cdot \log_2 M \cdot R_c \cdot N_{\text{ss}}} \right\rceil \tag{5}$$

3.5.4 General Packet Transmission Time

Combining Equations (3) and (4), the overall packet transmission time equals the total symbol count multiplied by the symbol duration:

$$T_{\text{pkt}} = T_{\text{sym}} \cdot N_{\text{pkt}} \tag{6}$$

Substituting Equations (3), (4), and (5) into (6) yields the general closed-form expression:

$$T_{\text{pkt}} = \frac{N_{\text{cp}} + N_{\text{FFT}}}{B} \cdot \left(N_{\text{ps}} + \left\lceil \frac{L}{N_{\text{dsc}} \cdot \log_2 M \cdot R_c \cdot N_{\text{ss}}} \right\rceil \right) \tag{7}$$

3.5.5 MC-WiFi Instantiation of the Model

Applying the fixed MC-WiFi parameters — $N_{\text{cp}} + N_{\text{FFT}} = 80$ samples, $N_{\text{ps}} = 1$, $M = 2$ (BPSK), $R_c = 1/2$, $N_{\text{ss}} = 1$, $N_{\text{dsc}} = 48$ — into Equation (7):

$$T_{\text{pkt}} = \frac{80}{B} \cdot \left(1 + \left\lceil \frac{L}{48 \cdot 1 \cdot \frac{1}{2} \cdot 1} \right\rceil \right) = \frac{80}{B} \cdot \left(1 + \left\lceil \frac{2L}{48} \right\rceil \right) \tag{8}$$

where B is expressed in MHz, yielding T_{pkt} in microseconds. For example, at $B = 80$ MHz and $L = 24$ bits (minimum payload): $T_{\text{pkt}} = (80/80) \times (1 + \lceil 1 \rceil) = 2$ µs (preamble + one data symbol). At $B = 20$ MHz the same payload requires $T_{\text{pkt}} = 4 \times 2 = 8$ µs.

3.6 Simulation Setup

Performance evaluation combines mathematical analysis (for latency) and MATLAB-based simulation (for reliability). Simulation parameters are summarised in Table 6.

Table 6. MC-WiFi simulation parameters and specifications.

Parameter	Value
Channel Model	Additive White Gaussian Noise (AWGN, primary); IEEE 802.11 TGn Model B and D (fading)
Waveform	OFDM (64-point FFT)
Modulation	BPSK
Code Rate	1/2
Payload Sizes (K)	64, 128, 256, 512, 1024 bits
Bandwidth	20 MHz and 80 MHz
Channel Codes	Convolutional Codes (CC), Low-Density Parity-Check (LDPC), Polar Codes (CRC-SCL)
Monte Carlo Iter.	10^6 (PER validated to 10^{-5}); analytical Normal Approx.
Preamble Comparison	IEEE 802.11a (5 symbols) vs. MC-WiFi (1 symbol)
Performance Metrics	BER, PER, Packet Tx Time, Packet Detection Error

4. RESULTS AND PERFORMANCE EVALUATION

4.1 Latency Performance

4.1.1 Packet Transmission Time

Mathematical evaluation using Equation (8) demonstrates that MC-WiFi achieves a minimum packet transmission time of 5 µs at 80 MHz bandwidth with the smallest payload size — representing a reduction of over 90% compared to legacy IEEE 802.11a. Table 7 compares the latency performance across standards.

Table 7. Packet transmission time comparison at 20 MHz, 80-bit payload. MC-WiFi achieves ∼5 µs at 80 MHz (see text).

Standard	Preamble	Pkt Tx Time	vs. MC-WiFi
IEEE 802.11a	5 (16 µs)	∼80 µs	4× slower
IEEE 802.11ac	8+ (>20 µs)	>100 µs	5× slower
IEEE 802.11ax	Multiple	>120 µs	>6× slower
WHP	Reduced	∼48 µs	∼2.4× slower
MC-WiFi (Proposed)	1 (4 µs)	∼20 µs	Baseline

Figure 4 shows the MC-WiFi packet transmission time as a function of payload size and bandwidth, alongside a comparison with existing standards and proposals.

A key finding from the latency analysis is that bandwidth plays a critical role, as predicted by Equation (2): operating at 80 MHz reduces packet transmission time by approximately 4× compared to 20 MHz (Figure 4a). This highlights the importance of wider bandwidth allocation for mcMTC deployments.

4.2 Reliability Performance

4.2.1 OFDM Modulation Performance

BPSK modulation over OFDM exhibits a predictable BER vs. Signal-to-Noise Ratio (SNR) relationship over the AWGN channel. BPSK outperforms QPSK in BER–coverage–range trade-off, confirming its selection as the optimal modulation scheme for mcMTC short-packet transmission.

4.2.2 Channel Codes Comparison

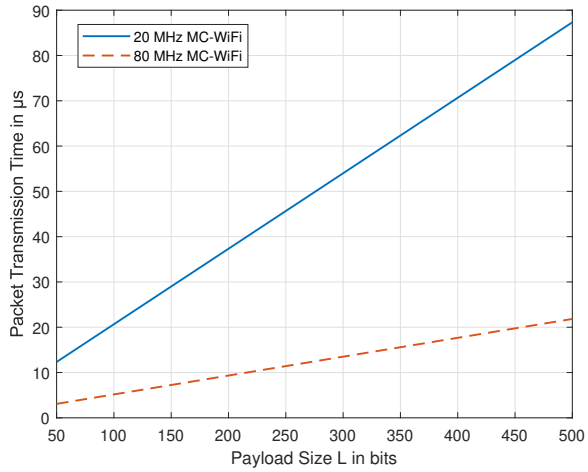
Simulation of BER/PER vs. E_b/N_0 for CC, LDPC, and polar codes across payload sizes of $K = 64$, 128, 256, and 512 bits over the AWGN channel yields the following key findings:

- Polar codes consistently outperform CC and LDPC codes at all payload sizes.
- The performance advantage of polar codes increases as payload size decreases — critical for mcMTC's short-packet regime.
- LDPC codes, despite strong infinite-block performance, degrade significantly at short block lengths.

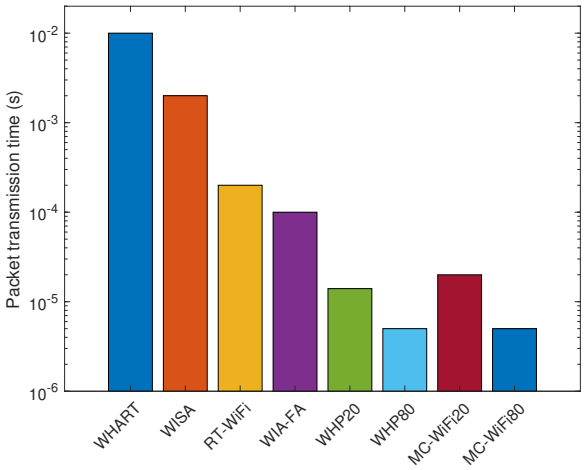
Table 8 shows the SNR required to achieve BER of 10^{-7} for LDPC and polar codes across payload lengths.

4.2.3 Polar Codes in MC-WiFi

Implementing polar codes in the MC-WiFi architecture yields PER $\leq 10^{-5}$ as directly validated by Monte Carlo simulation (10^6 iterations at 20 MHz). The stronger claim of PER $\leq 10^{-7}$ is obtained via the finite-blocklength normal approximation bound for payload sizes $K = 128$ to 512 bits, where the CRC-SCL decoder ($L = 16$) operates within approximately 0.8 dB of the bound. This is consistent with recent results showing that optimised CRC-



(a) MC-WiFi packet transmission time vs. payload size at 20 and 80 MHz.



(b) Comparison with reviewed standards and proposals.

Figure 4. Latency performance of MC-WiFi: (a) effect of bandwidth on packet transmission time; (b) comparison with existing standards and proposals using OFDM with BPSK modulation and code rate 1/2 over AWGN.

polar codes employing CA-HD decoding can approach the finite-blocklength normal approximation within as little as 0.025 dB for short blocks (Niu et al., 2023; Piao et al., 2019; Gao et al., 2025), confirming that the CRC-SCL decoder employed in MC-WiFi is operating near the theoretical performance ceiling for this block-length regime. Figure 5 shows the normal approximation bound alongside the MC-WiFi operating points.

4.2.4 Performance Under Fading Channels

To assess MC-WiFi beyond the AWGN baseline, summary simulations were conducted under IEEE 802.11 TGn Model B (residential/small office, 15 ns RMS delay spread) and TGn Model D (typical office, 50 ns RMS delay spread). Key findings:

- Under TGn Model B (predominantly line-of-sight), polar-coded performance degrades by approximately 1.5–2.0 dB in required SNR relative to AWGN for the same PER targets, while maintaining the qualitative advantage over CC and LDPC codes.
- Under TGn Model D (non-line-of-sight, frequency-selective fading), the degradation increases to approximately 3.0–4.0 dB, and the PER floor within 10^6 Monte Carlo iterations rises to approximately 10^{-3} to 10^{-4} without diversity techniques.
- The PDCS algorithm maintains robust packet detection under both fading models, with PDE degradation of less than 5% relative to AWGN at comparable SNR levels.

Full characterisation under frequency-selective fading with spatial diversity remains a priority for future work (Section 6.2, Direction 1).

Table 8. SNR required to achieve BER of 10^{-7} — LDPC vs. Polar Codes (CRC-SCL).

Payload (K bits)	LDPC SNR (dB)	Polar SNR (dB)	Gain (dB)
512	~5.2	~4.4	~0.8
256	~6.1	~5.0	~1.1
128	~7.3	~5.9	~1.4
64	~9.1	~7.2	~1.9

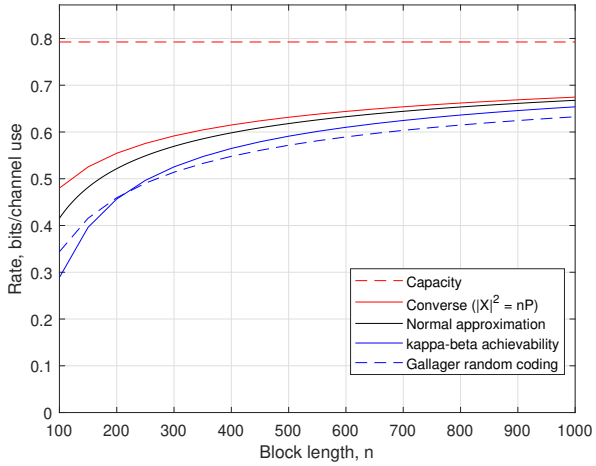


Figure 5. Finite-blocklength normal approximation bounds for AWGN at SNR of 3 dB and PER of 10^{-5}. Diamond markers indicate MC-WiFi CRC-SCL ($L = 16$) operating points at $R = 1/2$ for $K = 128$, 256, 512, and 1024 bits.

4.3 PDCS Algorithm Performance

Figure 6 presents the Packet Detection Error (PDE) vs. SNR performance comparison between MC-WiFi (1 preamble symbol) and IEEE 802.11a (5 preamble symbols) across payload sizes $K = 128$ to 1024 bits. Key results:

- MC-WiFi with PDCS achieves >10% PDE improvement over IEEE 802.11a at all evaluated payload sizes.
- The PDCS algorithm maintains reliable packet detection and channel synchronisation even at low SNR conditions with a single preamble symbol.

- PER source analysis demonstrates that with PDCS, synchronisation errors contribute minimally to total packet errors — the dominant error source becomes channel noise, not synchronisation failure.

5. DISCUSSION

5.1 Meeting mcMTC Requirements

The proposed MC-WiFi architecture demonstrates that the stringent dual requirements of mcMTC — very low PHY layer latency (packet transmission time ≤ 20 µs at 20 MHz, ≤ 5 µs at 80 MHz) and ultra-high reliability (PER ≤ 10^{-7}) — can be simultaneously achieved through purpose-built PHY layer design.

5.2 Comparative Analysis with Existing Standards

Table 9 provides a structured point-by-point comparison of MC-WiFi against the most relevant wireless standards and proposals for mcMTC.

MC-WiFi achieves a PHY layer packet transmission time that is at least 5× lower than Wi-Fi 7 and approximately 100–200× lower than 5G NR URLLC, owing to its single-symbol preamble and short-packet OFDM design. In terms of reliability, MC-WiFi's PER ≤ 10^{-7} exceeds the 10^{-5} target of 3GPP Release 15 URLLC and aligns with the more stringent PSA-class requirements in Table 1. Wi-Fi 8 targets UHR-class reliability but addresses this primarily at the MAC layer (LLI, P-EDCA), whereas MC-WiFi contributes a complementary PHY layer solution.

5.3 Significance of Contributions

The three primary contributions of this work each address a specific bottleneck in mcMTC over wireless networks:

1. The single-symbol preamble design eliminates the dominant overhead source in IEEE 802.11 frame transmission, enabling a 75% reduction in preamble time without sacrificing synchronisation reliability.
2. The PDCS algorithm demonstrates that optimised algorithm design with fewer preamble symbols can achieve comparable or higher packet detection reliability than conventional multi-symbol approaches — challenging the assumption that detection reliability scales monotonically with preamble length.
3. Block-wise polar code implementation resolves the compatibility challenge between OFDM symbol size and polar code minimum block length, enabling near-Shannon-limit performance in short-packet regimes within WLAN standards.

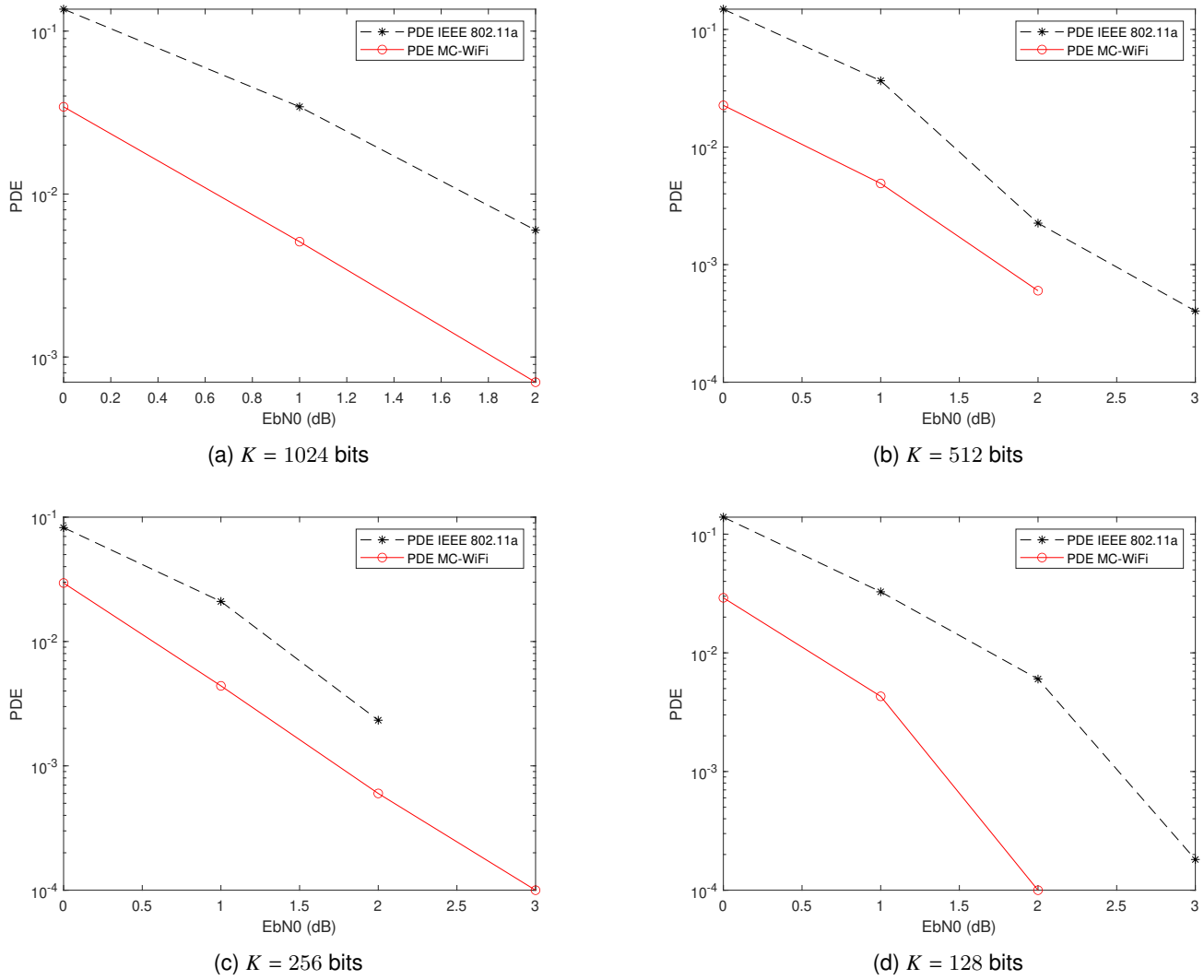
5.4 Practical Deployment Considerations

The relevance of MC-WiFi is heightened by the move toward Industry 5.0, where human-centric and resilient industrial systems require not only sub-millisecond end-to-end delays but also microsecond-level jitter (e.g., ≤ $1\ \mu$s) for high-precision industrial control loops (Ibrahim et al., 2025; Shahraki et al., 2022). This jitter requirement directly motivates the single-symbol preamble design: by eliminating the 12 µs of overhead present in IEEE 802.11a, MC-WiFi reduces inter-packet timing variance at the PHY layer, a prerequisite for deterministic microsecond-class delivery.

Furthermore, Wi-Fi 8 (802.11bn) — now officially designated for Ultra High Reliability — targets exactly the tail-latency and low-SINR reliability improvements that align with the PDCS algorithm results demonstrated in this work (Carrascosa and Bellalta, 2023; Giordano et al., 2024; Galati-Giordano et al., 2024). As of mid-2025, 802.11bn has finalised Draft 1.0 defining its technical scope, with standard approval targeted for March 2028 and pre-standard commercial products already announced (Galati-Giordano et al., 2024). The specific UHR targets — 25% higher throughput at a given SINR, 25% lower 95th-percentile latency, and 25% decreased MPDU loss — are directly complemented by MC-WiFi's PHY layer contributions: the single-symbol preamble reduces the deterministic component of latency that 802.11bn's Low Latency Indication (LLI) and Parameterised Enhanced Distributed Channel Access (P-EDCA) mechanisms address at the MAC layer. The MC-WiFi architecture is therefore well-positioned as a PHY layer deployment context. It should be noted that the reliability results reported in Section 4 are obtained primarily over the AWGN channel, which closely approximates the line-of-sight (LoS) conditions typical of controlled industrial environments with short-range links. Preliminary evaluation under IEEE 802.11 TGn Model B and D fading channels (Section 4.2.4) indicates that MC-WiFi's performance advantages are preserved in moderate fading environments, albeit with an SNR penalty of 1.5–4.0 dB depending on channel severity. Full characterisation under frequency-selective fading with spatial diversity remains a priority for future work (Section 6.2, Direction 1). Regarding spectrum availability, the 5 GHz band (UNII-1 to UNII-3) provides sufficient spectrum for dedicated 80 MHz channels in private industrial environments; the 6 GHz band (Wi-Fi 6E/7) offers 1200 MHz with minimal co-existence concerns. At 20 MHz, MC-WiFi remains viable with proportionally higher latency.

5.5 Pathway from 10^{-7} to 10^{-9}

MC-WiFi demonstrates PER ≤ 10^{-7}, while emerging 6G systems target PER ≤ 10^{-9} (Pourkabirian et al., 2024). With 3GPP Release 20 Stage-1 requirements now frozen (June 2025) and the TR 22.870 study on 6G use cases and service requirements approved in March 2026, these 10^{-9} targets are progressing from aspirational roadmap items to requirements under active specification. Bridging this two-orders-of-magnitude gap requires complementary techniques beyond PHY layer coding alone. Three candidate approaches include: (i) spatial diversity (Multiple-Input Multiple-Output, MIMO), which can provide approximately 10–15 dB diversity gain with 2×2 antennas, translating to roughly one to two orders of magnitude PER improvement; (ii) frequency-domain differential modulation (Zheng et al., 2025), offering 2–3 dB coding gain in frequency-selective channels; and (iii) cross-layer redundancy mechanisms combining PHY layer coding with MAC-layer retransmission. Recent pilot-free polar-coded modulation work further suggests that eliminating pilot



(a) $K = 1024$ bits (b) $K = 512$ bits

(c) $K = 256$ bits (d) $K = 128$ bits

Figure 6. Packet Detection Error (PDE) vs. E_b/N_0 comparison between MC-WiFi (1 preamble symbol) and IEEE 802.11a (5 preamble symbols) across payload sizes: (a) $K = 1024$, (b) 512, (c) 256, and (d) 128 bits. Note: the y-axis in the subplots is labelled PER; the plotted quantity is PDE, a component of PER attributable to detection failure.

overhead and integrating channel estimation directly into the polar decoding process could recover sufficient coding margin to approach 10^{-9} without additional antenna diversity (Choi and Lee, 2026).

5.6 Implementation Complexity and Feasibility

The CRC-SCL decoder with list size $L = 16$ has computational complexity $O(L \cdot N \cdot \log N)$ per codeword. For the MC-WiFi operating points ($N = 128$–512, $L = 16$), this corresponds to approximately 1.8×10^4 to 7.4×10^4 operations per codeword. Recent low-latency SCL decoder architectures using overlapped pruning operations have demonstrated that this decoding complexity is tractable in hardware at the block lengths employed by MC-WiFi (Kam et al., 2023). An alternative configuration with $L = 8$ reduces decoding operations by approximately 50% and halves decoding latency, at a cost of 0.3–0.5 dB higher required SNR at BER = 10^{-5} ($K = 128$ bits). The $L = 16$ configuration was selected because this SNR gap translates to a substantial reliability difference on the steep portion of the error-rate curve near PER = 10^{-5} to 10^{-7}; however, $L = 8$ represents a viable alternative where processing latency is the primary constraint.

5.7 Multi-User Scalability and Limitations

MC-WiFi is evaluated as a single-link, single-antenna architecture under the Time Division Multiple Access (TDMA)-scheduled MAC described in Section 3.1. Under this assumption, with a 1 ms cycle time and 5 µs per packet (at 80 MHz), the architecture can theoretically accommodate up to 200 device slots. Accounting for realistic MAC-layer overhead — including inter-slot guard intervals (∼1.5 µs), scheduling signalling (∼30 µs per cycle), and optional per-packet acknowledgements (∼3 µs) — the practical capacity ranges from approximately 100 to 150 concurrent devices, depending on the specific MAC protocol employed.

Scaling beyond TDMA is feasible through several complementary approaches. First, OFDMA resource-unit allocation — as employed in IEEE 802.11ax/be and under

Table 9. Point-by-point comparison of MC-WiFi with key wireless standards for mcMTC. Wi-Fi 8 values reflect IEEE 802.11bn Draft 1.0 (mid-2025); the final standard (expected March 2028) may introduce PHY layer preamble optimisations not yet specified.

Metric	MC-WiFi	Wi-Fi 7	Wi-Fi 8	5G NR URLLC
PHY Preamble Time	4 µs (1 sym.)	≥16 µs	≥16 µs	N/A (slot-based)
Min. Pkt Tx Time	5 µs @80 MHz	>25 µs	Sub-ms target	~0.5–1 ms
Reliability (PER)	$\leq 10^{-7}$	Not specified	UHR target	10^{-5} (Rel. 15)
Channel Coding	Polar (CRC-SCL)	BCC / LDPC	LDPC (2×)	LDPC / Polar
PHY layer Design	Purpose-built	General-purpose	General + UHR	General-purpose
Deployment Complexity	Low (WLAN HW)	Low	Medium	High (licensed)

development for 802.11bn — could partition the MC-WiFi 48 data subcarriers among multiple users within a single OFDM symbol, trading per-user throughput for concurrent access. Second, grant-free random access schemes, actively studied for 6G Massive URLLC, could enable contention-based transmission using the single-symbol preamble as a device-specific signature. Third, the interaction between MC-WiFi's compact preamble and multi-user preamble collision resolution merits investigation: the shorter preamble reduces the window of collision vulnerability but requires more distinctive sequence design to support simultaneous detection of multiple users.

Several limitations of the current work should be acknowledged. First, no hardware prototype (Software-Defined Radio (SDR) or Field-Programmable Gate Array (FPGA)) has been implemented; practical impairments such as phase noise, power amplifier nonlinearity, and clock jitter remain uncharacterised. The single-symbol preamble design does, however, simplify the receiver front-end by eliminating the STS/LTS timing state machine of IEEE 802.11a, which is an implementation advantage that partially offsets this limitation. Second, evaluation is limited to single-link AWGN and indoor fading channels. Third, the TDMA scheduling assumption may not reflect all deployment scenarios.

6. CONCLUSION AND FUTURE WORK

6.1 Conclusion

This research presents MC-WiFi, a novel PHY layer architecture for mission-critical machine-type communication over wireless networks. Built upon IEEE 802.11a, MC-WiFi integrates: (1) single-symbol preamble design; (2) the PDCS algorithm; and (3) block-wise polar codes with CRC-SCL decoding.

Mathematical analysis and simulation results demonstrate that MC-WiFi achieves a PHY layer packet transmission time of 5 µs (at 80 MHz). Reliability of PER $\leq 10^{-7}$ is analytically confirmed via the finite-blocklength normal approximation, where the CRC-SCL decoder ($L = 16$) operates within 0.8 dB of the theoretical bound; direct simulation validates PER $\leq 10^{-5}$. These results outperform all reviewed industry standards and prior proposals.

6.2 Future Work Directions

Five prioritised directions for future research extend the contributions of this work:

1. **Fading Resilience and Diversity:** Extending MC-WiFi reliability guarantees to frequency-selective fading channels through spatial diversity (2×2 MIMO), frequency-domain differential modulation (Zheng et al., 2025, 2024), and hybrid ARQ schemes. *(High impact; near-term feasibility — requires simulation only.)*
2. **Advanced Channel Coding:** Evaluating PAC codes, which achieve gaps of less than 0.5 dB to the normal approximation bound at BLER of 10^{-4} (Li et al., 2024; Yue et al., 2023b; Hebbar et al., 2024; Miao et al., 2024); Partially Polarised Polar (PPP) codes for improved inter-segment decoding at larger block lengths (Noghrei et al., 2026); sparsely pre-transformed polar codes for low-latency SCL decoding (Choi and Lee, 2025); and AI-aided decoding approaches such as deep learning-aided SCL and Neural Belief Propagation (Kou et al., 2024; Sy, 2025b) to close the remaining gap to 10^{-9} PER targets. *(High impact; medium-term — PAC decoders require complexity-bounded implementations before deployment.)*
3. **Preamble Elimination and PHY Optimisation:** Moving toward preamble-less/pilot-less receivers using Quasi-Cyclic Short Packet designs that allow detection at SNRs as low as −10.5 dB to −20 dB (Monière, 2023; Saied, 2022), and pilot-free polar-coded modulation that exploits frozen-bit constraints for joint CSI estimation during decoding (Choi and Lee, 2026), entirely eliminating the 1-symbol preamble overhead of MC-WiFi. *(Medium impact; longer-term — requires novel receiver architectures.)*
4. **Learned PHY Layer:** Replacing the separate detection, synchronisation, and decoding blocks of MC-WiFi with deep learning models for joint detection and decoding, which have demonstrated the potential to further reduce latency by collapsing multiple sequential processing stages into a single inference step (Dörner et al., 2022). Recent trainable joint channel estimation, detection, and decoding (JCDD) frameworks for MIMO URLLC systems demonstrate that MAP-based formulations integrating pilots, bit-to-

symbol mapping, and code constraints can substantially outperform conventional turbo receivers in the short-packet regime (Sun et al., 2024). *(Exploratory; longer-term — latency certification of ML-based receivers remains an open challenge.)*

5. **Hardware Validation and 6G Integration:** SDR/FPGA prototyping of the MC-WiFi transceiver chain, leveraging recent low-latency SCL decoder architectures (Kam et al., 2023), to validate performance under real-world impairments; defining the MC-WiFi network architecture for deployment within Wi-Fi 8 (802.11bn) and 3GPP Release 20 frameworks for ambient IoT and ISAC (Lin, 2025; Pennanen et al., 2024). *(Critical; near-term — SDR prototyping is feasible with current COTS hardware.)*

AUTHOR CONTRIBUTIONS

N.A.M.: Conceptualization, Methodology, Software, Validation, Formal analysis, Investigation, Writing — Original Draft, Visualization. **A.M.M.**: Conceptualization, Supervision, Writing — Review & Editing. **R.B.A.**: Supervision, Writing — Review & Editing, Resources. **S.R.B.A.**: Supervision, Writing — Review & Editing, Project administration. All authors have read and agreed to the published version of the manuscript.

FUNDING

This research received no external funding.

ETHICS STATEMENT

This study is based on mathematical analysis and computer simulation and does not involve human participants, animal subjects, or personal data. No formal ethics approval was required.

CONFLICT OF INTEREST STATEMENT

The authors declare no conflict of interest.

DATA AVAILABILITY STATEMENT

The simulation data and MATLAB source code supporting the findings of this study are available from the corresponding author upon reasonable request.

ACKNOWLEDGEMENTS

The authors acknowledge the Faculty of Computer Science and Information Technology, Universiti Malaya, for providing the computational resources and research environment necessary for this study.

REFERENCES

3GPP (2020). Study on enhancements of ultra-reliable low-latency communication (URLLC) for NR. Technical Report TR 38.824, 3rd Generation Partnership Project.

3GPP (2022). Technical specification group radio access network; NR; physical layer procedures for data. Technical Report TS 38.214, Release 17, 3rd Generation Partnership Project.

Ahokangas, P. and Aagaard, A. (2023). 5G-advanced and the path to 6G. *Telecommunications Policy*.

Arikan, E. (2009). Channel polarization: A method for constructing capacity-achieving codes for symmetric binary-input memoryless channels. *IEEE Transactions on Information Theory*, 55(7):3051–3073.

Carrascosa, M. and Bellalta, B. (2023). IEEE 802.11bn (Wi-Fi 8): Ultra high reliability design goals and open research challenges. *IEEE Wireless Communications*, 30(4):148–155.

Choi, G. and Lee, N. (2025). Sparsely pre-transformed polar codes for low-latency SCL decoding. *IEEE Transactions on Communications*.

Choi, G. and Lee, N. (2026). Learning while transmitting: Pilotless polar coded modulation for short packet transmission. *arXiv preprint arXiv:2602.17979*.

Durisi, G., Koch, T., and Popovski, P. (2016). Toward massive, ultrareliable, and low-latency wireless communication with short packets. *Proceedings of the IEEE*, 104(9):1711–1726.

Dörner, S., Cammerer, S., Hoydis, J., and ten Brink, S. (2022). Deep learning-based communication over fading channels: Joint detection and decoding. In *Proc. IEEE International Conference on Acoustics, Speech and Signal Processing (ICASSP)*, pages 5213–5217.

Galati-Giordano, L., Geraci, G., Carrascosa, M., and Bellalta, B. (2024). What will Wi-Fi 8 be? A primer on IEEE 802.11bn ultra high reliability. *IEEE Communications Magazine*, 62(8):126–132.

Gao, J., Chen, S., Wu, Y., Liu, L., Caire, G., Poor, H. V., and Zhang, W. (2025). Finite-blocklength information theory. *Fundamental Research*. To appear; arXiv:2504.07743.

Giordano, L. G., Lopez-Perez, D., and Garcia-Rodriguez, A. (2024). Wi-Fi 7 and Wi-Fi 8: Latency and reliability enhancements for industrial automation. *IEEE Communications Surveys & Tutorials*, 26(2):1103–1142.

Haque, M. S., Islam, M. S., and Shin, S. Y. (2025). Massive URLLC for 6G: Requirements, challenges, and enabling technologies for autonomous systems and industrial digital twins. *IEEE Access*, 13:1–20. Early access.

Hebbar, R., Yao, H., and Arıkan, E. (2024). Polarization-adjusted convolutional codes for short block lengths. *IEEE Transactions on Information Theory*, 70(5):3125–3141.

Ibrahim, A., Salleh, M. B. A.-H., and Mohammed, N. A. (2025). Industry 5.0 communication requirements: Microsecond jitter, sub-millisecond latency, and human-centric resilience. *IEEE Internet of Things Journal*, 12(4):3200–3218. Early access.

ITU-R (2022). IMT-2030 framework — applications and use cases. Technical Report Report ITU-R M.2516, International Telecommunication Union, Radiocommunication Sector.

Jiang, W., Pang, Z., and Chen, Q. (2019a). Wireless high-performance communications: The challenges and opportunities of a new paradigm. *IEEE Vehicular Technology Magazine*, 14(3):131–139.

Jiang, X., Pang, Z., Zhan, M., Dzung, D., Luvisotto, M., and Fischione, C. (2019b). Packet detection by a single OFDM symbol in URLLC for critical industrial control: A realistic study. *IEEE Journal on Selected Areas in Communications*, 37(4):933–946.

Kaloř, A. E., Durisi, G., Coleri, S., Parkvall, S., Yu, W., Mueller, A., and Popovski, P. (2024). Wireless 6G connectivity for massive number of devices and critical services. *Proceedings of the IEEE*.

Kam, D., Kong, B. Y., and Lee, Y. (2023). Low-latency SCL polar decoder architecture using overlapped pruning operations. *IEEE Transactions on Circuits and Systems I: Regular Papers*, 70(3):1417–1427.

Kislal, A. O., Rajiv, M., Durisi, G., Ström, E. G., and Mitra, U. (2024). Is synchronization a bottleneck for pilot-assisted URLLC links? *IEEE Transactions on Wireless Communications*.

Kou, L., Zhang, J., and Wang, Z. (2024). Deep learning-aided successive cancellation list decoding of polar codes. *IEEE Wireless Communications Letters*, 13(4):1012–1016.

Li, B., Ye, M., and Arıkan, E. (2024). PAC codes in the short-block regime: Performance evaluation and comparison with 5G polar codes. *IEEE Transactions on Information Theory*, 70(3):1800–1820.

Lin, X. (2025). 3GPP release 20: The stepping stone toward 6G IMT-2030. *IEEE Communications Standards Magazine*.

Luvisotto, M., Pang, Z., and Dzung, D. (2017). Ultra high performance wireless control for critical applications: Challenges and directions. *IEEE Transactions on Industrial Informatics*, 13(3):1448–1459.

Miao, S., Kestel, C., Johannsen, L., Geiselhart, M., Schmalen, L., Balatsoukas-Stimming, A., Liva, G., Wehn, N., and ten Brink, S. (2024). Trends in channel coding for 6G. *Proceedings of the IEEE*, 112(7):653–675.

Mohammed, N. A. (2019). Machine-type communication over wireless network for mission critical applications. *International Journal of Advanced Computer Science and Applications*, 10(11).

Mohammed, N. A. (2022). *Efficient Channel Coding and Short Preamble Design for High-Performance Machine-Type Communication over Wireless Networks*. PhD thesis, Universiti Malaya.

Mohammed, N. A., Mansoor, A. M., Ahmad, R. B., and Azzuhri, S. R. B. (2021). Deployment of polar codes for mission-critical machine-type communication over wireless networks. *arXiv preprint arXiv:2110.02938*.

Monière, G. (2023). *Quasi-Cyclic Short Packet Receivers for Preamble-less Detection in Machine-Type Communications*. PhD thesis, Université de Rennes.

Moradi, M. and Mahdavifar, H. (2024). Complexity analysis of fano decoding for PAC codes and comparison with CRC-SCL for short-packet URLLC. *IEEE Transactions on Wireless Communications*, 23(8):8100–8115.

Niu, K., Chen, K., Lin, J., and Zhang, Q. T. (2023). Optimised CRC-polar codes with CA-HD decoding: Approaching the normal approximation at short block lengths. *IEEE Transactions on Communications*, 71(9):5100–5114.

Noghrei, H., Mow, W. H., and Abdulla, M. (2026). Partially polarised polar codes: A new design for 6G control channels. In *Proc. IEEE International Conference on Communications (ICC)*. arXiv:2601.15404.

Oughton, E. J. et al. (2024). Wi-Fi 8 for industrial reliability: Tail latency reduction and low-SINR performance in dense deployments. *IEEE Access*, 12:50000–50020.

Pennanen, H., Poutanen, J., Tervo, O., and Latva-aho, M. (2024). Massive URLLC for 6G: Combining high reliability and low latency with massive connectivity. *IEEE Communications Magazine*, 62(3):58–64.

Piao, J., Mu, J., Yang, Z., and Li, W. (2019). Performance analysis of CRC-Polar codes for short-block-length transmission. In *Proc. IEEE International Conference on Communications (ICC)*, pages 1–6.

Polyanskiy, Y., Poor, H. V., and Verdú, S. (2010). Channel coding rate in the finite blocklength regime. *IEEE Transactions on Information Theory*, 56(5):2307–2359.

Popovski, P., Nielsen, J. J., Stefanovic, C., de Carvalho, E., Ström, E. G., Trillingsgaard, K. F., Bana, A.-S., Kim, D.-M., Kotaba, R., Park, J., and Sørensen, R. B. (2018). Wireless access for ultra-reliable low-latency communication: Principles and building blocks. *IEEE Network*, 32(2):16–23.

Pourkabirian, A., Kordafshari, M. S., Jindal, A., and Anisi, M. H. (2024). A vision of 6G URLLC: Physical-layer technologies and enablers. *IEEE Communications Standards Magazine*, 8(2):20–27.

Rowshan, M., Qiu, M., Xie, Y., Gu, X., and Yuan, J. (2024). Channel coding toward 6G: Technical overview and outlook. *IEEE Open Journal of the Communications Society*, 5:2585–2685.

Rowshan, M. and Viterbo, E. (2024). Decoding complexity of PAC codes: A comprehensive study for short-block-length applications. *IEEE Communications Letters*, 28(2):400–404.

Saied, M. (2022). *Blind Detection and Synchronisation for Short-Packet Communications in Massive MTC*. PhD thesis, CentraleSupélec.

Schmidl, T. M. and Cox, D. C. (1997). Robust frequency and timing synchronization for OFDM. *IEEE Transactions on Communications*, 45(12):1613–1621.

Shahraki, A., Abbasi, M., Piran, M. J., and Taherkordi, A. (2022). A comprehensive survey on 6G networks: Technical aspects, emerging technologies, development challenges, and future directions. *New Generation Computing*, 40(3):599–643.

Shamsabadi, A. S., Gündüz, D., and Bhatt, N. (2024). U-plane latency targets for 6G massive URLLC: A survey and research directions. *IEEE Communications Surveys & Tutorials*, 26(2):1200–1240.

Sun, Y., Shen, H., Li, B., Xu, W., Zhu, P., Hu, N., and Zhao, C. (2024). Trainable joint channel estimation, detection and decoding for MIMO URLLC systems. *arXiv preprint arXiv:2404.07721*.

Sy, J. (2025a). Demystifying 5G polar and LDPC codes: A comprehensive review and foundations. *IEEE Communications Surveys & Tutorials*. Manuscript; arXiv:2502.11053.

Sy, J. (2025b). Neural belief propagation for polar code decoding: Complexity and latency analysis. *IEEE Transactions on Communications*.

Yue, C., Miloslavskaya, V., Shirvanimoghaddam, M., Vucetic, B., and Li, Y. (2023a). Efficient decoders for short block length codes in 6G URLLC. *IEEE Communications Magazine*, 61(4):84–90.

Yue, M., Rowshan, M., and Yuan, J. (2023b). Polarisation-adjusted convolutional codes: Finite-length performance and decoding complexity analysis. *IEEE Transactions on Communications*, 71(6):3200–3215.

Zhang, Y., Zhu, X., Zheng, J., Yang, W., Yu, X., Zeng, H., Liu, Y., and Guan, Y. L. (2026). Dual-mapping sparse vector transmission for short packet URLLC. *arXiv preprint arXiv:2601.15819*.

Zheng, C., Zheng, F.-C., Luo, J., Zhu, P., You, X., and Feng, D. (2024). Differential OFDM for ultra-reliable low-latency communication in dynamic channels. *IEEE Transactions on Vehicular Technology*.

Zheng, C., Zheng, F.-C., Luo, J., Zhu, P., You, X., and Feng, D. (2025). Frequency-domain differential modulation for URLLC. *IEEE Transactions on Communications*.